A Detailed Comparative Analysis between two Soft Switching techniques used in PV Applications

Anup Anurag, *Student Member*, *IEEE,* Satarupa Bal, *Student Member, IEEE*, and B. Chitti Babu, *Member, IEEE*
Department of Electrical Engineering, National Institute of Technology, Rourkela-769 008 (INDIA)
E-mail: anup.rana123@gmail.com, bal.satarupa03@gmail.com, bcbabunitrkl@ieee.org

***Abstract*— This paper presents a detailed comparative study between two different soft switching techniques used in PV applications. An extended range ZVS active clamped current fed full-bridge isolated boost converter has been studied and the comparison has been done with a soft switching boost converter using an auxiliary resonant circuit. The former uses the energy stored in the leakage inductance of the transformer and its magnetizing inductance to perform the soft switching whereas the latter uses a resonant circuit in order to carry out the same. A typical 500 W converter is employed to investigate both the converters. Comparisons have been made on the basis of operating modes and range of operation. Detailed operation, analysis and simulation results for the designs have been presented. The systems are modeled and simulated in PSIM 64 bit version 9.0 Environment.**

Keywords— Zero Voltage Switching, Zero Current Switching, DC-DC converter, Photovoltaic (PV) array

I. INTRODUCTION

With the spurt in the use of conventional energy sources, the possibility of their exhaustion and environmental pollution is aggravating. Also global energy consumption is growing exponentially. Thus the very low environmental impact of the renewable energy sources makes them a very attractive solution for a growing demand. Renewable sources of energy include solar energy, wind energy, geo-thermal energy, tidal energy etc. Among these alternative sources of energy, despite their relatively high cost, the electrical energy from photovoltaic is currently regarded as the prerequisite sustainable resource for both stand alone as well as grid connected applications, since it offers zero input fuel cost, abundant and clean and distributed over the Earth [1].

Nevertheless, this kind of intermittent power generation usually causes problems in the electrical system it is connected to, because of the lack or scarcity of control on the produced active and reactive power. This requires assessment of PV power potential and selection of appropriate PV Module. Several studies have been directed world over on characterization of PV data and site matching of solar energy [2-4]. It is also observed from literature that mathematical models of few individual components of PV system are represented and simulated for better understanding of their performances [5].

The major component that affects the accuracy of the simulation is the PV cell modeling which involves the estimation of the I-V and P-V characteristics curves. Various mathematical models such as Simplified Single Diode Model (SSDM), the Single Diode Model (SDM), the two diode model and also three diode model are proposed in literature [6]-[8]. Simulations have helped the process of developing new systems including power converter, by reducing cost and time. Simulation tools have the capabilities of performing dynamic simulations of such system in a visual environment so as to facilitate the development of new systems. To maximize the efficiency of PV Panel and other renewable sources of energy, apart from hard switching, various soft switching techniques are being proposed. Zero Voltage Switching (ZVS), Zero Current Switching (ZCS) and Zero Current Transition (ZCT) are the techniques used where switches are turned on or turned off under zero voltage and zero current condition. Various methods for soft switching to maximize the efficiency have been proposed in literature [9]-[11]. In this paper, an active-clamped current-fed-full-bridge dc-dc converter is discussed and analyzed with wide range of ZVS operation [12]. The magnetizing inductance of transformer aids to the efficiency to the converter at light load condition maintaining the duty cycle to 50% which is the most necessary condition for this methodology. Also, a soft switching boost converter using an auxiliary resonant circuit is analyzed and discussed owing to simplified circuit design [13]. However, during closed loop control ZVS isn't maintained for wide range of load variation. Further, a typical 500W converter is employed to investigate both the converters performance. Comparisons have been made on the basis of operating modes and range of operation. Detailed operation, analysis and simulation results for the designs have been presented.

The organization of the paper is as follows. Section II depicts the mathematical analysis for the active clamped current fed full-bridge isolated boost converter. Section III describes the mathematical analysis for the soft switching boost converter using an auxiliary resonant circuit. Section IV describes the comparative analysis and simulation results and Section V concludes the paper followed by the references.

II. MATHEMATICAL ANALYSIS OF ACTIVE CLAMPED CURRENT FED FULL-BRIDGE ISOLATED BOOST CONVERTER

In order to analyse the different operational modes of the converter the following assumptions are made:

- The input voltage is constant
- Output capacitance is large enough to obtain constant output voltage
- Main inductor is large enough to have input current constant
- All components are ideal

The auxiliary capacitor is large enough to maintain constant voltage across it.

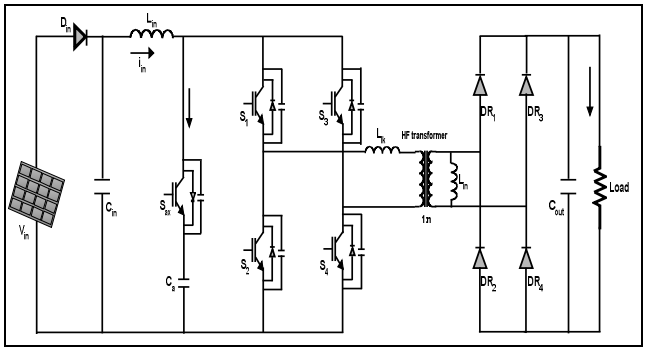

Fig.1. Active Clamped Current Fed Full-Bridge Isolated boost converter

Figure 1 illustrates the active clamped current fed full-bridge isolated boost converter. The operational modes of the proposed converter are divided into nine modes and the operational modes are illustrated in figure 2.

Mode 1(t_0-t_1) – In the beginning of this stage, the auxiliary switch S_{ax} is off and all the main switches S_1~S_4 are on. The power transfer to the load is done by the energy stored in the capacitor. Input inductor starts storing energy. The transformer magnetizing current circulates through its leakage inductance.

Mode 2(t_1-t_2) - In this mode, main switches S_2 and S_3 are turned off. The input current now flows through the path provided by the auxiliary circuit. This causes zero current in the main switches. The magnetizing current flows through the antiparallel diodes D_1 and D_4 and through the leakage inductance.

Mode 3(t_2-t_3) - In the beginning of this mode, there is an increase in the main switch voltages. A positive voltage is seen across the leakage inductance of the transformer and the current rises linearly. Rectifier diodes start conducting when the leakage inductance current goes above the magnetizing current reflected to primary side. Power is transferred to load.

Mode 4(t_3-t_4) – Here, in this mode the antiparallel diode of the auxiliary switch starts conducting thus making the voltage across the switch to be zero. Current through the main switches change their direction.

Mode 5(t_4-t_5) – In this mode, the auxiliary switch gets turned on with ZVS. Magnetizing current increases with the same slope as before. At the end of this mode, the current through the auxiliary capacitor reaches its negative peak.

Mode 6(t_5-t_6) - In the beginning of this mode, the auxiliary switch is turned off. The leakage inductance current charges the auxiliary capacitor. At the end of the interval capacitors C_2 and C_3 discharge to a particular value.

Mode 7(t_6-t_7) - In this mode, the charging of the auxiliary capacitor still continues and C2 and C3 are discharged. At the end of this interval C2 and C3 discharge to zero and the auxiliary capacitor charges to its initial value.

Mode 8(t_7-t_8) – In this mode, the antiparallel body diodes D_2 and D_3 starts conducting thus making the voltage across them to be zero. The switches are ready for ZVS turn on. The interval ends when the leakage inductance current equals the input current.

Mode 9(t_8-t_9) - In this mode, the switches are turned on by ZVS. The leakage inductance current flows through switches S_2 and S_3. The end of the mode is marked by the leakage impedance current being equal to the magnetizing current reflected to primary side.

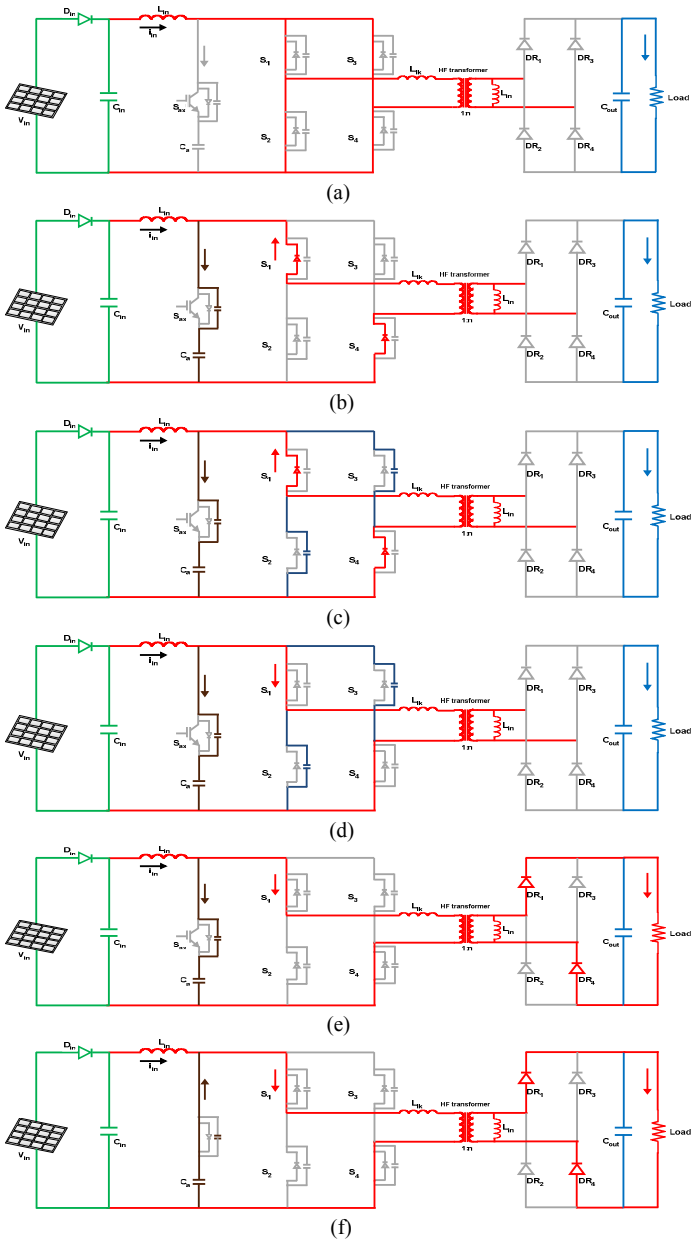

(a) (b) (c) (d) (e) (f)

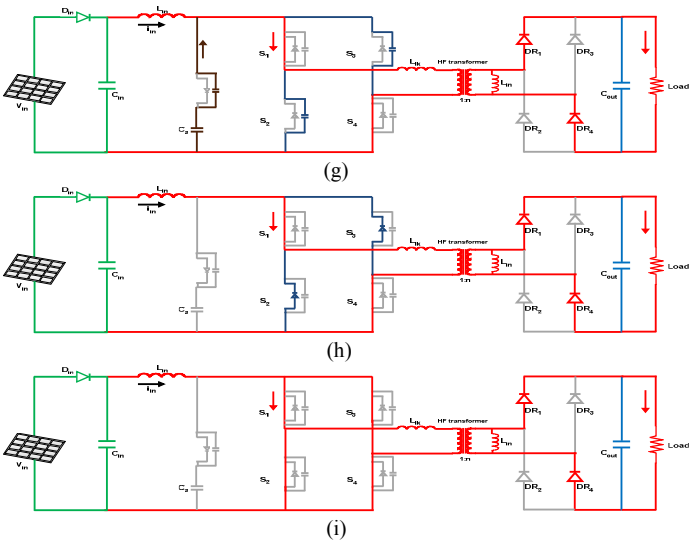

Fig. 2. Equivalent circuits of (a) Mode 1 (b) Mode 2 (c) Mode 3 (d) Mode 4 (e) Mode 5 (f) Mode 6 (g) Mode 7 (h) Mode 8 (i) Mode 9

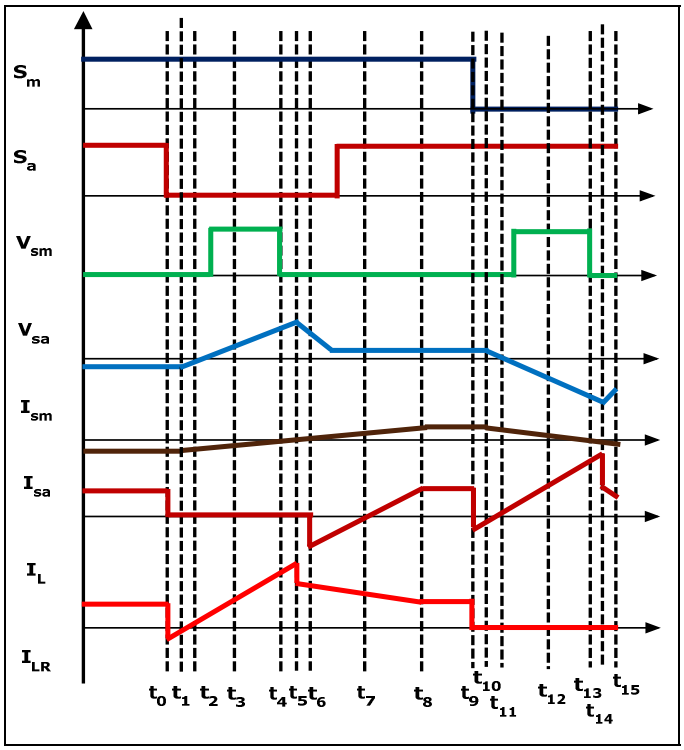

Fig.3. Waveforms for the Active Clamped Current Fed Full-Bridge Isolated boost converter

III. Mathematical Analysis Of Soft Switching Boost Converter Using An Auxiliary Resonant Circuit

Analysis of the converter is based on three assumptions:

- *The input voltage is constant*
- Output capacitance is large enough to obtain constant output voltage
- Main inductor is large enough to have input current constant

Fig. 4 illustrates the soft switching boost converter using an auxiliary resonant circuit. Here in addition to the conventional boost converter, an additional resonant circuit is incorporated. The operational modes of this converter are divided into nine modes and the operational modes are illustrated in fig 5.

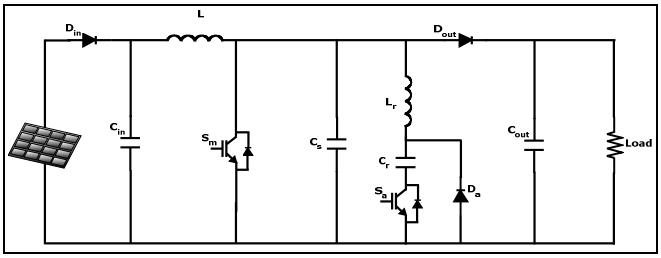

Fig.4. Soft Switching Boost Converter topology using an auxiliary resonant circuit

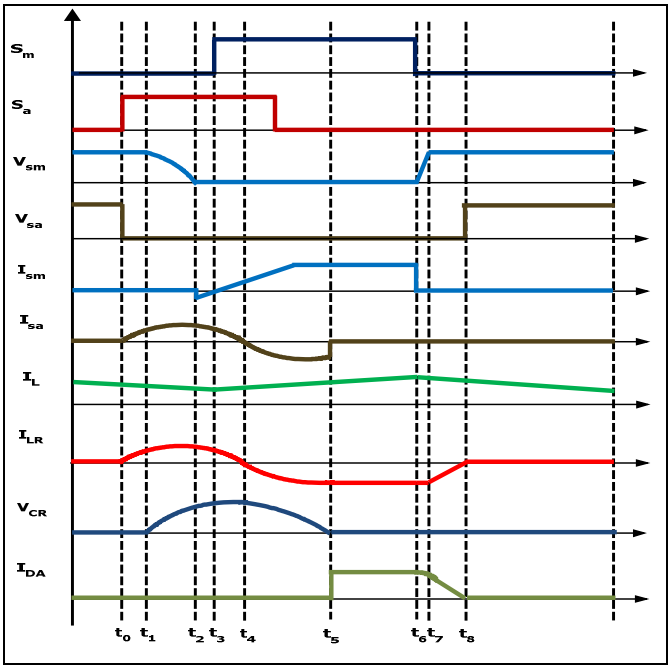

Fig.5. Waveforms of the soft switching converter using an auxiliary resonant circuit

Mode 1(t_0-t_1) - At the beginning of this stage, auxiliary switch S_a is turned on with ZCS while the main switch is off. A resonant loop of L_m-L_r-C_r-S_a-V_{in} is formed because of the resonance between L_r and C_r. The current in D_1 reaches zero at the end of the interval. Thus, if the current of L_m is equal to L_r, mode 1 ends. The voltages and currents are derived using KVL and KCL. The power loss in this interval is due to the conduction loss due to switch S_a and main diode D_{out}.

Mode 2(t_1-t_2) - At this interval, switch S_a is still on and the current through L_r increases due to the resonance between L_r and C_r. The drain voltage of main switch S_m starts to drop as the snubber capacitor discharges. This mode ends when the voltage of C_r drops to zero. The power loss in this mode is mainly due to the conduction loss in the switch S_a.

Mode 3(t_2-t_3) - At the beginning of this interval, the anti-parallel diode of main switch S_m is turned on which makes the

voltage across main switch zero (ZVS). This mode ends when the main inductor current is same as that of the resonant inductor current. The power loss in this mode is due to the conduction loss of both switch S_a and the anti-parallel diode of switch S_m.

Mode 4(t_3-t_4) - Here, the main switch S_m is turned on at zero voltage condition and hence, there is no switching loss across it. The resonant capacitor is charged continuously in this mode. The power losses in this interval include conduction loss in main switch S_m as well as auxiliary switch S_a.

Mode 5(t_4-t_5) - The current flows through the anti-parallel diode of S_a. Hence, the switch S_a is turned off under ZVS. This mode ends when resonant capacitor C_r is fully charged. Thus, there is no switching loss in S_a during turn-off. The power loss in this interval is due to the conduction loss across switch S_m and the anti-parallel diode of switch S_a.

Mode 6(t_5-t_6) - In this interval, the current flows through the auxiliary diode D_a instead of the anti-parallel diode of switch S_a. This mode ends when the main switch S_m is turned off. Here, the power loss is influenced by the switching loss of the auxiliary diode D_a and the conduction loss across switch S_m and D_a.

Mode 7(t_6-t_7) - In this mode, the main switch S_m is turned off under ZVS condition by the help of snubber capacitor. The energy is stored in the capacitor C_s. This mode ends when C_s is fully charged. Thus, the switching loss across S_m is zero and the entire loss is contributed by the conduction loss of D_a.

Mode 8(t_7-t_8) - Here the resonant inductor L_r starts discharging and the energy is transferred to the load through the output diode (D_{out}). This mode comes to an end when L_r is discharged completely. Because of the ZVS condition, D_{out} doesn't experience any switching loss and thus the power loss is due to the conduction loss across D_a and D_{out}.

Mode 9(t_8-t_9) - In this interval, all the switches are turned off and the entire current flows through the D_{out} to the load. Hence this mode ends when S_a is turned on. The power loss is contributed by the switching loss of D_a and the conduction loss of D_{out}.

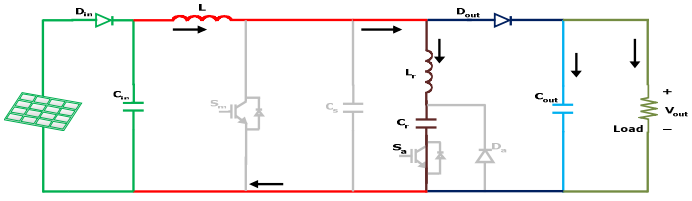

(a)

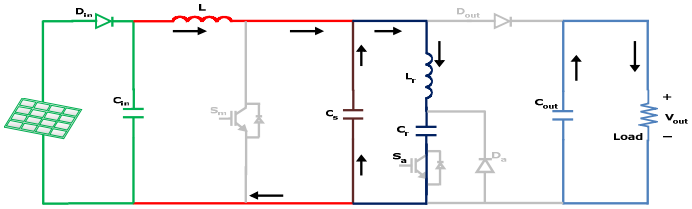

(b)

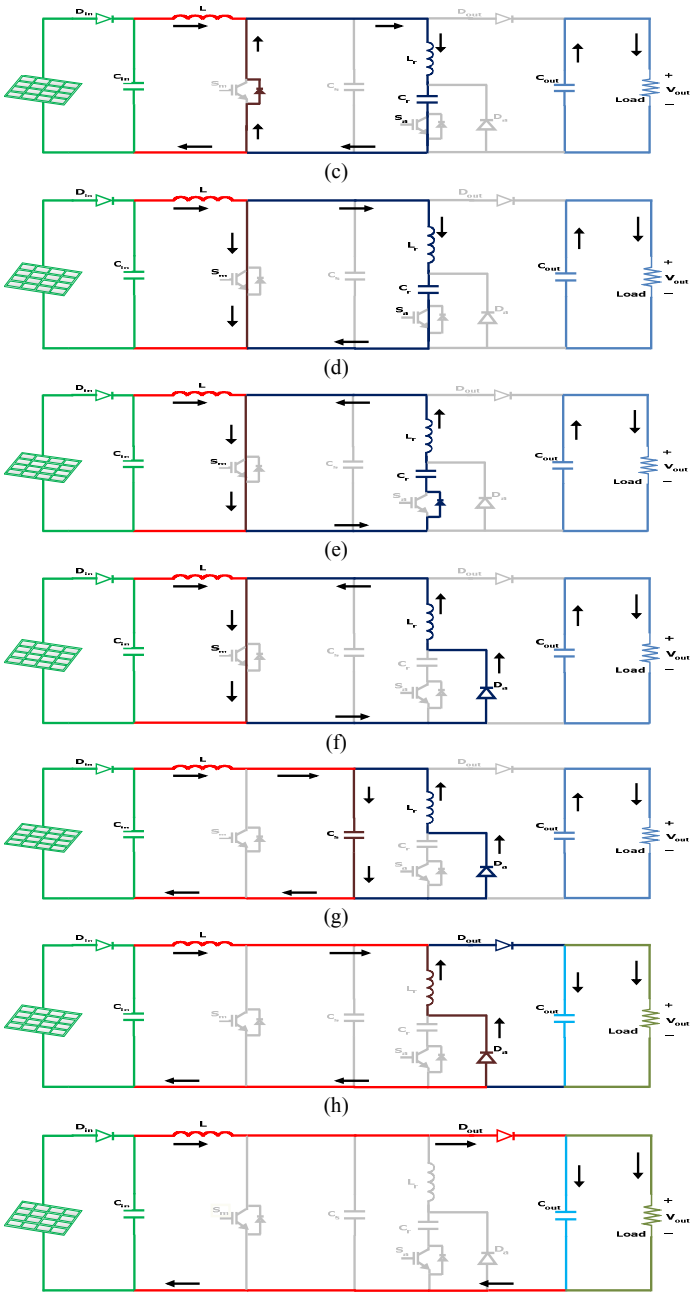

(c) (d) (e) (f) (g) (h) (i)

Fig.6. Equivalent circuits of (a) Mode 1 (b) Mode 2 (c) Mode 3 (d) Mode 4 (e) Mode 5 (f) Mode 6 (g) Mode 7 (h) Mode 8 (i) Mode 9

IV. RESULTS AND DISCUSSIONS

The designed boost converters along with the PV panel and a control tracker for MPPT algorithm is simulated using PSIM 64 bit version 9.0.

A. Analysis of the Active Clamped Current Fed Full-Bridge Isolated boost converter

Table 1 shows the values of all the parameters used in the simulation and design of the converter. A small signal model of PV Panel is assumed with output power maintained at 500W.

TABLE I
PARAMETERS USED IN SIMULATION

Parameter	*Label*	*Value*
Output Voltage	V_{out}	350 V
Rated Power	P_{rated}	500 W
Main inductor	L	132 uH
Leakage inductance	L_{lk}	0.4 uH
Turns on secondary side of HF transformer	N	8
Auxiliary Capacitor	C_{ax}	4 uF
Switching Frequency	f_{sw}	100,000 Hz
Output Capacitor	C_{out}	4.9 nF
Ripple Factor	$R.F.$	25 %

Simulation results have been shown in fig. 7. The main switch and auxiliary switch voltage as well as current waveforms in fig. 7(b) to fig. 7(f) shows the ZVS turn on and turn off.

These results are shown for full load conditions. The switching pulse to the main switches S_1 and S_4 is identical and S_2 and S_3 is same. ZVS occurs across the main switches and the auxiliary switch since the anti-parallel diodes conducts before the gating signal is applied to the switches. Voltage across the transformer and leakage inductance as shown in figure (7) encounters for ZCS of rectifier diodes.

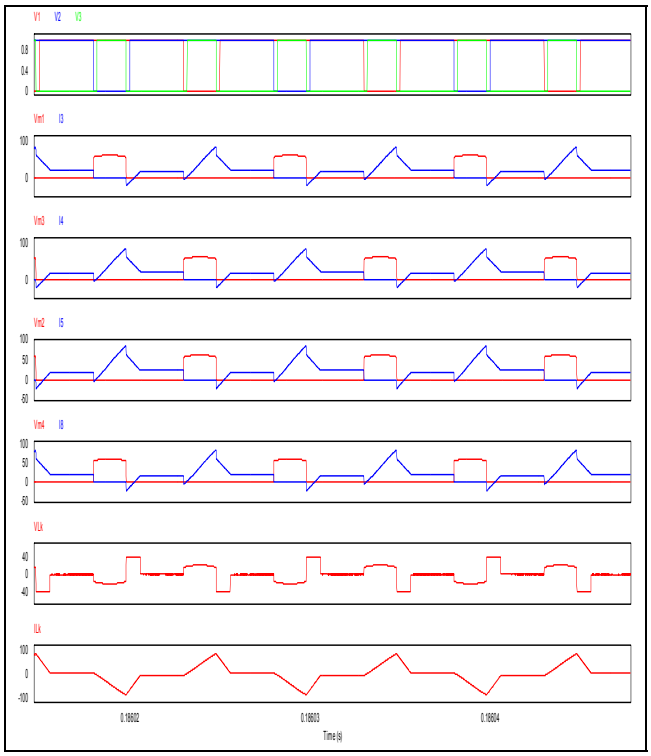

Fig. 7. Simulation waveforms : (a) Gating Signals to main switch and auxillary switch ,(b) Voltage and Current through main switch S1 , (c) Voltage and Current through main switch S2, (d) Voltage and Current through main switch S3, (e) Voltage and Current through main switch S4, (f) Voltage and Current through auxillary switch Sax, (g) transformer Volatge V_{AB} and (h) Leakage Inductor Current I_{LK}

B. *Analysis of the Soft Switching Boost Converter topology using an auxiliary resonant circuit*

Table 2 shows the values of all the parameters used in the simulation and design of the converter.

TABLE II
PARAMETERS USED IN SIMULATION

Parameter	*Label*	*Value*
Output Voltage	V_{out}	350 V
Rated Power	P_{rated}	500 W
Main inductor	L	5.6 mH
Resonant Inductor	L_r	50 uH
Resonant Capacitor	C_r	500 nF
Snubber Capacitor	C_s	100 nF
Switching Frequency	f_{sw}	100,000 Hz
Input Capacitor	C_{in}	4.9 nF
Ripple Factor	$R.F.$	25 %

Simulation results have been shown in Fig. 8. The main switch voltage and current waveforms in Fig. 8(b) and Fig. 8(c) shows the ZVS turn on and turn off. The anti-parallel diode and the parasitic capacitor ensures Zero Voltage before turning of the switch.

The auxiliary switch voltage and current waveforms have been shown in fig. 8(c). The resonance between the inductor and the capacitor and the reversing of the inductor current leads to the turn on of the switch by ZCS. The anti-parallel diode present is responsible for the ZVS turn off of the auxiliary capacitor. The current through the input inductor which was assumed to be constant, has a small amount of ripple present which has been accounted for.

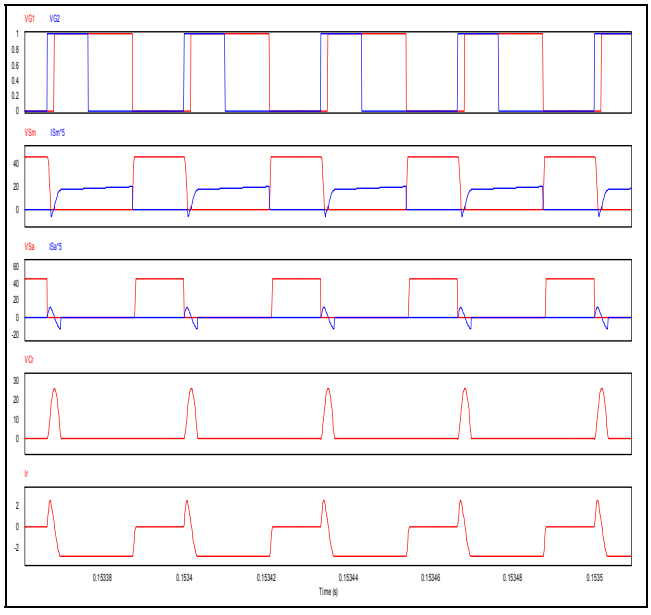

Fig. 8. Simulation waveforms : (a) Gating Signals ,(b) Voltage and Current across main switch ,(c) Voltage and Current across auxiliary switch, (d) Voltage across resonant Capacitor and (e) Current through resonant inductor L_r

C. *Comparative Analysis*

With prior knowledge of the analysis, the two soft switching schemes are compared. Here open-loop control of the converter is employed assuming small-signal modeling of the PV Panel. The Active Clamped Current Fed Full-Bridge Isolated boost converter is successful in maintaining high efficiency for varying load conditions. Fig. 9 shows the comparative analysis between the two which markedly elaborates the higher efficiency of the Active Clamped Current Fed Full-Bridge Isolated boost converter where ZVS is maintained in both the converters. The increase in leakage current from magnetizing inductance during light load condition results in the increase in efficiency compared to later method. However, at full load condition both the methods illustrate same efficiency.

There are some limitations following up the former method. If the ratio L_{lk}/L_m is imperfect, the duty ratio turns out to be less than 50% and hence, isn't suitable for light load condition. Thus, this converter has a limitation of main switch's duty cycle should always be greater than 0.5. Further, the use of a HF transformer and a number of MOSFET's/IGBT's and diodes makes the circuit more complex and also encounters more switching loss during light load condition if ZVS isn't maintained.

The Soft Switching Boost Converter topology using an auxiliary resonant circuit which incorporates the design of the conventional boost converter with just an additional resonant circuit for soft switching applications suffers from no such limitations. However, it doesn't offer ZVS for a wide range of load variations during closed loop control which leads to decrease in efficiency at lower percentage of loads. During open-loop control, the light load is unable to draw current and hence the switching loss appears to be prominent thus, reducing the efficiency.

We can thus say that even if the control circuit for the Active Clamped Current Fed Full-Bridge Isolated boost converter is more complex, it provides adequate leeway for the loads and thus makes it more useful than the Soft Switching Boost Converter topology using an auxiliary resonant circuit. At places where we have a fixed load, owing to the circuit complexity, the latter serves the purpose better.

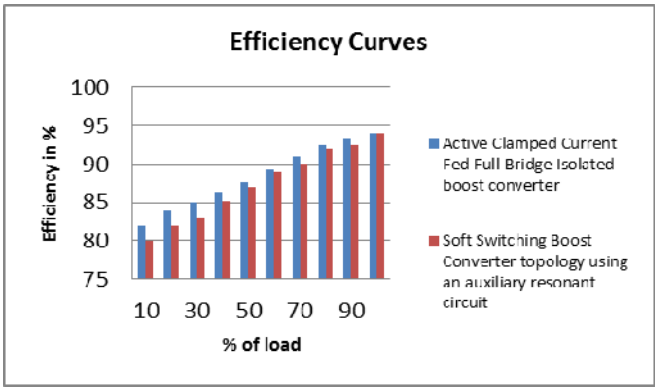

Fig.9. Variation in efficiency of the converters with changes in the percentage of load applied

V. CONCLUSIONS

This paper presents a comparative study between two soft switching techniques on the basis of their efficiencies load variations and power losses. A small signal model of PV Panel was considered for the open-loop control of their converters. Thus, ZVS was maintained for a wide range of load variation for both the methods. Amongst the two schemes, the pros and cons of each of them were discussed and it was found that the Active Clamped Current Fed Full-Bridge Isolated boost converter served better when there is light load condition keeping the duty cycle more than 50% all the time.

However, the later method proved to be less complex as compared to the former when there is a fixed load present. At full load condition i.e. 100% load both the methods shows same efficiency of the converter. But during closed loop control, ZVC is difficult to maintain for wide range of load for this method. This can be useful in determining the appropriate technique when the use of boost converter is considered for efficient use of PV panel.

REFERENCES

[1] M.A.G. Brito, L.G. Junior, L.P. Sampaio, C.A. Canesin."Evaluation of MPPT Techniques for Photovoltaic Applications", in Proc. International Symposium on Industrial Electronics - ISIE, 2011.

[2] S. Jain, and V. Agarwal, "An integrated hybrid power supply for distributed generation applications fed by nonconventional energy sources," *IEEE Transactions on Energy Conversion*, vol. 23, no.2, June 2008, pp. 622-631.

[3] Anup Anurag, B.Chittii Babu, "Control of Grid Connected Inverter for Sinusoidal Current Injection with improved performance", In. p*roc*. 1st IEEE Students' Conference on Engineering & Systems (SCES 2012), MNNIT, Allahabad, Mar/2012.

[4] Bose, B.K.; , "Need a Switch?," Industrial Electronics Magazine, IEEE vol.1, no.4, pp.30-39, Winter 2007

[5] M. H. Todorovic, L. Palma and P. Enjeti, "Design of a wide input range DC-DC converter with a robust power control scheme suitable for fuel cell power conversion," *IEEE Trans on Industrial Electronics*, vol. 55, 2008, pp. 1247-1255.

[6] Z. Salam et al., "An improved two-diode photovoltaic (PV) model for PV system," in Proc. Joint Int. Conf. Power Electron., Drives and Energy Syst., India, 2010, pp. 1–5.

[7] M. G. Villalva et al., "Comprehensive approach to modeling and simulation of photovoltaic arrays," IEEE Trans. Power Electron., vol. 24,no. 5, pp. 1198–1208, May 2009.

[8] G. R. Walker, "Evaluating MPPT converter topologies using a matlab PV model," J. Elect. Electron. Eng., vol. 21, pp. 49–55, 2001, Australia

[9] F. J. Nome, and I. Barbi, "A ZVS clamping mode-current-fed push pull DC-DC converter," In P*roc. IEEE International Symposium on Industrial Electronics (ISIE* 1998) 1998, pp. 617-621.

[10] A. K. Rathore, A. K. S. Bhat, and R. Oruganti, "A comparison of soft-switched DC-DC converters for fuel cell to utility interface application', *IEEE Transactions on Industry Applications*, vol. 128, No. 4, 2008, pp. 450-458.

[11] H. Tao, A. Kotsopoulos, J. L. Duarte, and M. A. M. Hendrix, "Transformer-coupled multiport ZVS bidirectional DC–DC Converter with wide input range," *IEEE Transactions on Power Electronics*, vol. 23, March 2008, pp. 771-781.

[12] Prasanna, U.; Rathore, A.; , "Extended Range ZVS Active-Clamped Current-Fed Full-Bridge Isolated Dc/Dc Converter for Fuel Cell Applications: Analysis, Design and Experimental Results," *IEEE Transactions on Industrial Electronics*, , Vol. 59,No:12., pp.1, 2012

[13] I. Song, D. Jung, Y. Ji, S. Choi, Y. Jung, and C. Won, "A Soft Switching Boost Converter using an Auxiliary Resonant Circuit for a PV System", in IEEE ECCE'11 Conf. Proc., 2011, pp. 2838-2843